

Compositional and structural investigation of HCN polymer through high resolution mass spectrometry



Jean-Yves Bonnet^a, Roland Thissen^{a,*}, Maëli Frisari^a, Véronique Vuitton^a, Éric Quirico^a, François-Régis Orthous-Daunay^a, Odile Dutuit^{a,c}, Léna Le Roy^{b,1}, Nicolas Fray^b, Hervé Cottin^b, Sarah M. Hörst^d, Roger V. Yelle^e

^a UJF-Grenoble 1/CNRS-INSU, Institut de Planetologie et d'Astrophysique de Grenoble (IPAG) UMR 5274, Grenoble F-38041, France

^b Laboratoire Interuniversitaire des Systèmes Atmosphériques (LISA), UMR CNRS 7583, Université Paris Est Créteil et Université Paris Diderot, Institut Pierre Simon Laplace, Créteil, France

^c Space Research Institute, Austrian Academy of Science, Graz, Austria

^d Cooperative Institute for Research in Environmental Sciences (CIRES), Boulder, CO, USA

^e Lunar and Planetary Laboratory (LPL), Tucson, AZ, USA

ARTICLE INFO

Article history:

Received 17 April 2013

Received in revised form 19 June 2013

Accepted 21 June 2013

Available online 1 July 2013

Keywords:

HCN polymers

Composition

Structure

Mass spectrometry

MS/MS

ABSTRACT

Nitrogen rich compounds are found in numerous planetary environments such as planetary atmospheres, meteorites and comets. To better understand the structure and composition of this natural organic material, laboratory analogs have been studied. Though HCN polymers have been studied since the beginning of the 19th century, their structure and composition are still poorly understood. In this work we report the first extended high resolution mass spectrometry study of HCN polymers. The mass spectra of the polymer contain hundreds of peaks to which we try to assign an elemental composition. Elemental analysis has been used to constrain the molecular formulae and isotopic signatures have also been used to confirm them. The large quantity of amine functions observed with both infrared (IR) spectroscopy and mass spectrometry indicates that amine groups are present in most chains found in HCN polymer. Collision induced dissociation (CID) tandem (MS^n) measurements were also performed on eight molecular ions and aromatic rings have been identified.

© 2013 Elsevier B.V. All rights reserved.

1. Introduction

HCN polymers are complex polymeric materials, composed of carbon, nitrogen and hydrogen. They have been scrutinized for a long time because such materials are suspected to be present on a wide variety of solar system objects and beyond [1–4]. HCN polymers and other complex nitrogenated organics are believed to potentially form in the cometary environment [5], on the surface of icy satellites in the outer solar system [6–8], and in planetary atmospheres [9,10]. For example it has been suggested that they are present in Titan aerosol analogs, so-called Titan tholins (complex CHN containing material produced by RF discharges in N_2/CH_4 gas mixture) [11] although it has been shown that they only represent a minor fraction of tholins [12]. It has also been proposed that HCN polymers make up part of the refractory organic fraction of comets and they probably constitute a solid reservoir that releases

gaseous CN producing a CN distributed source in cometary atmospheres [13–15]. However their presence has not been confirmed yet by laboratory analyses of cometary grains, even though nitrile signatures have been observed by IR and XANES (X-ray absorption near edge structure) spectroscopy of Stardust particles [16].

Both HCN and NH_3 have been detected in cometary environment [17,18] and in the laboratory, pure HCN polymers result from the direct polymerization of HCN molecules, which can be hastened by addition of a base such as ammonia (NH_3). HCN polymers exhibit a large variety of properties, solubilities and compositions. They are thus a family of solids rather than a pure and reproducible polymer [19]. The study of HCN polymer is complicated by difficulties in controlling the experimental conditions, which is the major source of heterogeneity between samples. HCN polymers are reactive and they hydrolyze to form prebiotic molecules such as amino acids and even polypeptides [20–26]. Although such compounds (HCN polymers) are of great interest in various planetary issues and were first observed more than 200 years ago (by Proust 1806 and by Gay-Lussac in 1815), they have never been analyzed by high resolution mass spectrometry (HRMS). IR and NMR spectroscopies provide a glimpse into the polymeric structure and show that HCN polymers are relatively simple in terms of chemical diversity [12,27–30]. A

* Corresponding author. Tel.: +33 684344253.

E-mail address: roland.thissen@obs.ujf-grenoble.fr (R. Thissen).

¹ Present address: Center for Space and Habitability, University of Bern, Sidlerstrasse 5, CH-3012 Bern, Switzerland.

Table 1
Elemental analysis of HCN polymer in weight percentages and derived N/C and H/C ratios. As the oxygen is only a trace element, oxygen has not been included when assigning the molecular formulae. Relative errors are typically of 1%.

	C (wt%)	N (wt%)	H (wt%)	O (wt%)	H/C (atomic)	N/C (atomic)	O/C (atomic)
First analysis	43.2 ± 1	52.5 ± 1	4.3 ± 1	Absent or traces	1.19 ± 0.20	1.04 ± 0.002	0
Second analysis	43.1 ± 1	52.6 ± 1	4.3 ± 1	Absent or traces			

recent and detailed study by He et al. [31] used multidimensional NMR spectroscopy to investigate the structure of HCN polymers. Discrete structural units for small molecular components have been identified (with abundant presence of primary amines, bound to sp² carbon). A polyimine chain-like structure is proposed for the polymer, resulting from nucleophilic addition to form C–C bonds.

We report here the first extended HRMS study of HCN polymer seeking to explore their chemical structure and composition in order to identify some of the molecular structures. This work follows the comparison of HCN polymers and Titan tholins by HRMS presented in Vuitton et al. [12] and the first HRMS work on tholins performed by Somogyi and co-workers [32]. In this paper, we will also draw the attention to the intrinsic complexity observed within a given sample of HCN polymer. The HCN polymer used in this study was synthesized at the Laboratoire Interuniversitaire des Systèmes Atmosphériques (LISA, Créteil, France).

Detlef Schroeder, who was a good friend of some authors of the present paper, has produced, throughout his prolific career, very innovative results related to the extra-terrestrial chemistry. Let us cite his works related to the potential chemistry in Titan ionosphere [33–36] which are perfect illustrations of the scientific anthems that he developed: innovation and quality.

2. Materials and methods

2.1. Samples

Numerous methods have been proposed to synthesize HCN polymer (see [12] and references within). In our case, it was produced by the direct polymerization of HCN molecules mixed with 10% ammonia as previously described by Matthews and Moser in 1967 [24]. Due to its toxicity, HCN is not a commercial product. Therefore pure HCN must be synthesized before producing a polymer.

In our case, HCN is produced by the reaction between NaCN (Aldrich 98%) and stearic acid (CH₃(CH₂)₁₆COOH, Merck, 97%). The two powders are introduced in equimolar proportions in a vacuum manifold maintained at low pressure (<10⁻⁵ mbar) for a few hours in order to remove all the adsorbed water and trapped air. The mixture is heated to 350 K under dynamic vacuum to melt the stearic acid and drive the acid/base reaction between stearic acid and CN⁻, resulting in the production of sodium stearate, HCN gas and traces of CO₂ and formic acid (HCOOH). The resulting gases are then collected and condensed in a trap cooled to the temperature of liquid nitrogen (77 K). The ice is then slowly heated to 140 K to sublimate trace impurities in the ice except HCN, which remains frozen at those temperature and pressure conditions (<10⁻⁵ mbar). The sample purity is checked using IR spectroscopy and the main contaminant is found to be formic acid (HCOOH) in a minor abundance.

Polymerization is performed as follows: HCN and NH₃ (Air Liquide 99.995%) are mixed at room temperature in a sealed flask in proportions of HCN:NH₃ = 10:1 at room temperature. Since the polymerization reaction is exothermic, the flask is kept at room temperature in a water bath, to prevent a temperature increase. In the flask, NH₃ is mostly gaseous and HCN is mostly liquid. At the equilibrium, the reactive liquid is composed of HCN, NH₃, NH₄⁺ and CN⁻. As the reaction occurs, a solid appears slowly in the flask. Its

color evolves from yellow to orange, to brown and finally to black. We let the reaction progress for 51 days and collect the resulting black powder after pumping all the volatiles still present in the flask.

2.2. Analytical techniques

2.2.1. Elemental analysis

Elemental analyses of HCN polymers used in this study were obtained by combustion for C, N and H simultaneously and by pyrolysis for O. The very limited oxygen content was checked by pyrolysis as oxygen can be involved in the polymerization reaction due to residue of formic acid (HCOOH) in the pure HCN. The measured C, N, H and O mass percentages are shown in Table 1, along with the N/C, H/C and O/C elemental ratios.

2.2.2. Infrared spectroscopy

Infrared spectra were acquired using a Fourier transform Hyperion 3000 infrared microscope (Bruker), operating in the range 700–3800 cm⁻¹ with a spectral resolution of 4 cm⁻¹. The samples were crushed onto a diamond window. The spectra were acquired under high vacuum (<10⁻⁵ mbar) to minimize the contribution of adsorbed water. Each spectrum is the average of 200 individual scans.

2.2.3. Mass spectrometry

The HCN polymers used in this study were dissolved in methanol with an initial concentration of 1 mg mL⁻¹, followed by 30 min sonication. The solid is almost completely soluble in pure methanol. Nevertheless the samples were centrifugated at 9000 × g for 3 min in order to clearly separate the liquid from the small fraction of remaining solid. The supernatant was then introduced into an LTQ-Orbitrap XL mass spectrometer (Thermo Fischer Scientific) equipped with the Ion Max ElectroSpray Ionization (ESI) source which was used with a spray voltage of 3.5 kV in positive ionization mode and 3.7 kV in negative ionization mode. The tube lens voltage was maintained at 50 V (–50 V in the negative mode) and the transfer tube was heated to 275 °C. The sample was infused into the ionization system by flow infusion at a rate of 3 μL min⁻¹. External calibration of the Orbitrap was performed daily using the manufacturer's Calmix calibration solution in the mass range *m/z* = 200–2000.

Full scan mode mass spectra were acquired using a mass range from *m/z* = 50–1000 divided into two subranges of *m/z* = 50–300 and *m/z* = 150–1000. The lowest mass accessible in high resolution with the Orbitrap is 50 Da. Full mass spectra correspond to the average of roughly 300 spectra collected in 10 min. The Orbitrap has a resolving power (*m/Δm*) better than 10⁵ up to *m/z* = 400. With this resolving power we are able to measure the exact mass of each ionizable molecule of the solution with accuracy better than 5 ppm (on average 2 ppm). This high resolution and accuracy allows for the use of the exact mass to attribute the molecular formulae. The mass defect is a powerful tool to constrain the molecular formulae as only one combination of C, N and H can reproduce the mass defect within 5 ppm in the whole mass range considered in this study. Tandem mass spectrometry (MS/HRMS) was also performed on HCN polymers using a strict and repetitive protocol in the LTQ ion trap, using helium as the activation gas and final mass analysis

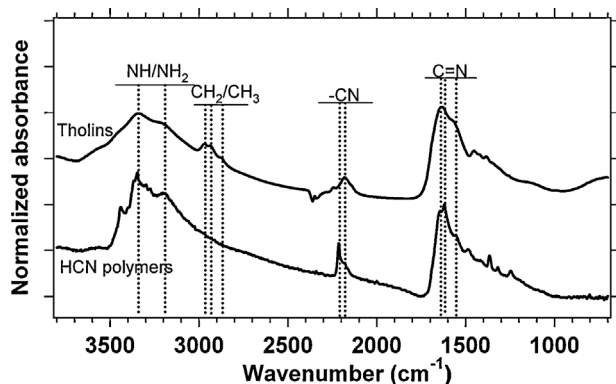


Fig. 1. Infrared spectra of HCN polymers and, for comparison, tholins produced from 90:10 N_2 : CH_4 mixture. The HCN polymers spectrum exhibits strong amine and nitrile signatures, a more complex feature below 1650 cm^{-1} composed of $\text{C}=\text{N}$ and possible ring contributions and no clear methyl mode.

being performed in the Orbitrap. The normalized collision energy was set to 30% (the absolute collisional energy is not known) with an activation time of 30 ms and an isolation window of 1.2 Da. In this technique, ions (parent ions) within the isolation window are selected in the LTQ ion trap, and their internal energy is increased by collision with He, until the weaker bonds are broken, producing specific ions (daughter ions). In our case, this technique allows measuring the exact masses of the neutral fragment, as the final products are measured in the Orbitrap (high resolution mass analyzer). Using the LTQ, specific daughter ions can be selected and further fragmented iteratively. This repetitive fragmentation has been applied five times consecutively starting from the parent ion at $m/z = 244$ ($\text{C}_9\text{H}_{10}\text{N}_9^+$). This iterative process is ultimately limited by the availability of signal. MS/MS spectra correspond to the average of 5 min of acquisition.

Data acquisition was performed using the LTQ Tune Plus software (Thermo Fischer Scientific) and data processing was performed using custom software developed at the Lunar and Planetary Laboratory (University of Arizona) and at the Institut de Planétologie et d'Astrophysique de Grenoble (France). Molecular formulae were calculated assuming that no oxygen is present in the sample.

3. Results and discussion

3.1. Elemental analysis

The elemental analysis, in weight percentages, of HCN polymer allows us to derive the C/H, C/N and C/O ratios as summarized in Table 1. The verified low abundance of oxygen allows us to calculate molecular formulae containing only C, N and H atoms and demonstrates the high level of purity of the HCN polymer with very little contamination or remaining pollution coming from the synthesis protocol. From the C/H and C/N ratios we can derive an atomic excess of 19% for hydrogen and 4% for nitrogen both with respect to carbon in a pure HCN polymer in which the C/N and C/H can be thought to be equal to 1. This excess represents less than 3 wt% of the whole polymer.

3.2. Infrared spectroscopy

A typical infrared spectrum of HCN polymers is shown in Fig. 1. As a comparison a spectrum of tholins, a solid composed of H, C and N, initially designed to study Titan's atmosphere aerosols, recorded on the same instrument is also displayed. Tholins are produced by Pampre experiment [37]. Though not all the spectral bands are fully understood, the HCN polymer spectrum shows prominent amine

and nitrile features. The amine band is composed of numerous contributions with some of them potentially attributable to hydrogen bound amines (around 3190 cm^{-1}) and other to free amines (no hydrogen bond) around 3350 cm^{-1} . No clear methyl (CH_2 , CH_3) features are visible. The nitrile band around 2200 cm^{-1} is composed of two clear contributions that were described in Carrasco and co-workers [38]. The most intense feature in this region can be assigned to (or at least are consistent with) nitriles linked to aromatic ring at 2215 cm^{-1} and the second feature at 2180 cm^{-1} can be assigned to nitriles linked to unsaturated chains. A complex feature is visible at 1650 cm^{-1} and below. This feature is composed of the signatures of different chemical functional groups, mainly $\text{C}=\text{N}$ and amine bending modes, with the possible contribution of ring structures. These spectra clearly demonstrate the relative simplicity of HCN polymers in terms of chemical diversity as their infrared features are relatively sharp compared to the broad bands of tholins.

3.3. High resolution mass spectrometry (HRMS)

HRMS has been demonstrated to be a suitable technique for the analysis of complex organics such as tholins and HCN polymers [12,39]. ESI-HRMS enables an analysis of complex organics without previous separation or derivatization, and therefore provides a snapshot of all the molecules that are readily soluble and ionizable in the initial material. ESI is a soft ionization method that does not fragment molecules and reveals them as protonated positive ions or deprotonated negative ions. The resolving power and dynamic detection range of the Orbitrap, allow us to access the isotopic signature (^{13}C and ^{15}N) of intense ions in addition to their mono-isotopic peaks in the spectra. For the sake of clarity, isotopic signatures are treated in a dedicated part of the results section, and all the other representations contain only mono-isotopic (i.e. corresponding to the most abundant natural isotope of ^{12}C , ^{14}N , ^1H) signatures. Let us mention that ESI is known to produce sometimes sodium adducts instead of protonated ions. The precision of measurements in the low mass region and the positive assignment of ions without any sodium inclusion led us to rule out this kind of adduct in ESI ions from HCN polymers. In this section, the general description of the spectrum will be the first step to the analysis of the molecular content of our HCN polymer. The assigned molecular formulae and their relationship will be used as a cornerstone to identify major compounds in the polymer, and their fragmentation behavior will be analyzed to identify some molecular structures.

3.3.1. General description of the mass spectrum and molecular formulae assignment

Fig. 2 represents the global mass spectrum of HCN polymers (normalized intensities versus mass to charge ratio) between $m/z = 50$ and 1000 in positive ion mode (panel A) and in negative ion mode (panel B). The ionization method does not fragment molecules and therefore each spectral peak corresponds to a unique molecular formula but could correspond to multiple isomers. Evaluation of the mass distribution of molecules in the polymers shows that the signal is dominated by 20 intense peaks while the majority of the peaks have much lower intensities in both positive and negative modes. HCN polymer ions were successfully detected from the mass 55.0286 ($\text{C}_2\text{H}_3\text{N}_2^+$) to the mass 996.3792 ($\text{C}_{37}\text{H}_{34}\text{N}_{37}^+$) with maximum intensities below $m/z = 400$ representing a cumulative intensity of 82% of the whole signal and the assigned peaks have intensities between 0.01 and 2.5×10^6 counts (between 1×10^{-6} and 1 in normalized intensities) for the positive spectrum. For the negative spectrum HCN polymer ions were detected from 53.0150 ($\text{C}_2\text{H}_1\text{N}_2^-$) to 601.2905 ($\text{C}_{22}\text{H}_{29}\text{N}_{22}^-$) also with maximum intensities below $m/z = 400$, representing a cumulative intensity of 92% of the whole signal and

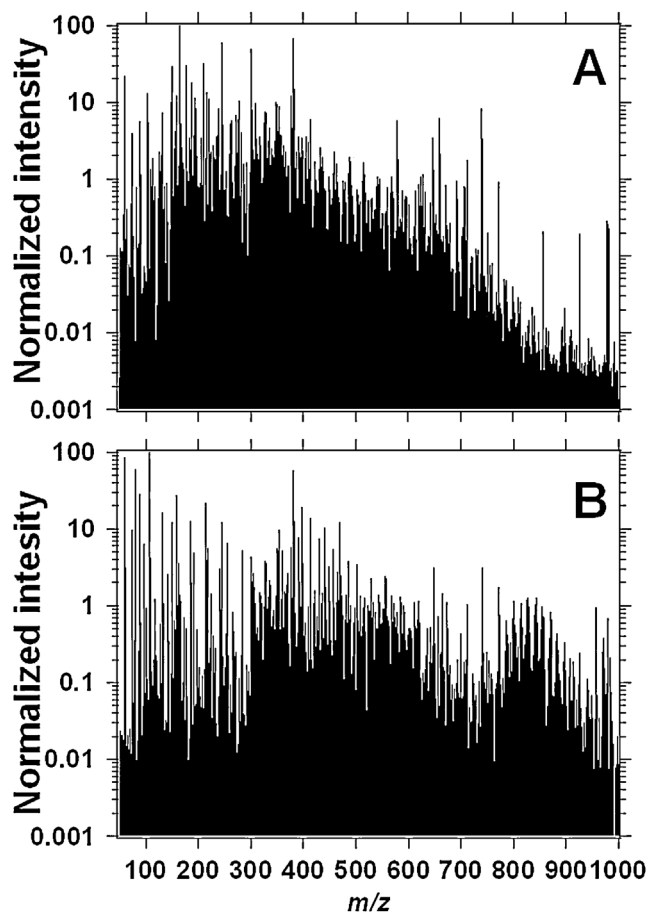


Fig. 2. Mass spectrum of HCN polymer in positive ion mode (panel A) and in negative ion mode (panel B). These spectra show that ions were present from $m/z=50$ –1000 and the general molecular mass distribution throughout the mass range. The signal is dominated by 20 intense peaks, but the majority of the peaks have low intensities.

the assigned peaks have intensities between 8.77 and 1.3×10^7 counts (between 6×10^{-7} and 1 in normalized intensities). This represents a dynamic range for ion detection better than 10^6 . Fig. 3A shows the evolution of the mass defects, i.e. the decimal fractions of the exact mass (shown as black squares) for all the measurements (raw spectrum, before molecular formula calculation) in positive mode. Three clear groups of mass defects are observed, the first corresponds to HCN polymers, the second corresponds to doubly charged ions (of HCN polymers) and the third corresponds to contamination (or molecular noise, i.e. species that are present in the environment of the mass spectrometer and arise in the spectrum, though they are not present in the solution). This contamination is also present in the blank spectra. Fig. 3A and B show also the mass defects of the peaks that have been assigned to a molecular formula (light blue triangles, representing 4.5% of the total number of peaks in positive mode and 23% in negative mode and about 90% of the cumulative intensity in both modes) and three simulated mass defect evolutions of pure polymeric CH_2 polymer ($(\text{CH}_2)_x$: red circles), pure HCN polymer ($(\text{HCN})_x$: blue dots) and HCNO polymer ($(\text{HCNO})_x$: red triangles). The CH_2 and HCNO patterns were chosen because of their extreme mass defect tendencies (high and low mass defects respectively), compared to the HCN polymer. The molecular assignment (i.e. passage from the ion mass to the molecular formula) is based on the exact mass measurement and the mass defect. As the exact masses of the ions are measured with a very high resolution ($\geq 10^5$ up to $m/z=400$) and a very good accuracy (within 2 ppm), the mass defect is a direct function of the mass defects of the atoms building the ion. Then by combining

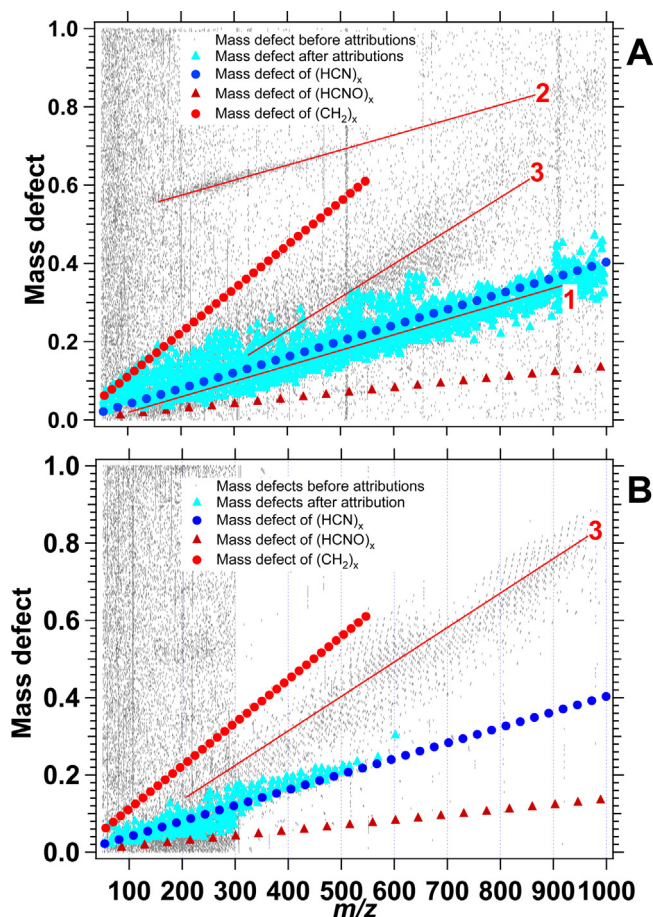


Fig. 3. Mass defects (i.e. the decimal fraction of the exact mass) of all the identified peaks in the positive ion mass spectrum (panel A). Trend 1 corresponds to HCN polymers, trend 2 to doubly charged ions and trend 3 to contamination. The mass defects of the assigned molecular formulae (light blue triangles) and simulated mass defects of CH_2 polymer (red circles), HCN polymer (blue circles) and HCNO polymer (red triangles) are also shown. Mass defects of all the identified peaks in the negative ion mass spectrum (panel B). The smaller extent of the identified HCN molecules is clearly visible (light blue triangles). Trend 1 corresponds to HCN polymers and trend 2 to contamination. The mass defects of the assigned molecular formulae (light blue triangles) and simulated mass defects of CH_2 polymer (red circles), HCN polymer (blue circles) and HCNO polymer (red triangles) are also shown. (For interpretation of the references to color in this figure legend, the reader is referred to the web version of this article.)

atomic mass defects of carbon, nitrogen and hydrogen we are able to calculate theoretical mass defects and to compare them with the measured ones. As a good agreement is found between theoretical and measured mass defects (<2 ppm) the assignment is taken into account. The spectra are, prior to assignment, internally calibrated using exact masses of molecules that are unambiguously present in the polymer see [39] for more details about formulae assignment. The identified molecular formulae resemble the evolution of HCN polymer-like mass defects, plus a few molecules that we attribute to molecular noise. The same representation is also displayed in Fig. 3B for the negatively charged ions. The same distribution of mass defects is observed with two major differences: (i) no multiply charged ions can be observed and (ii) smaller extent (in mass, no assignments above $m/z=600$) of the negatively ionized HCN polymer molecules. The distribution of the molecular mass defects, around the simulated pure HCN polymer mass defect evolution, is due to the diversity of molecules present in the real sample. This shows that our method of molecular formula calculation is efficient enough to separate the real HCN polymer molecules from the noise (electronic and contamination) and

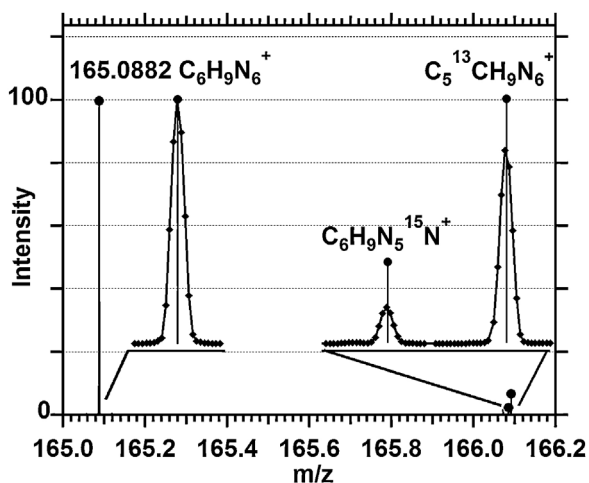


Fig. 4. Isotopic validation of the assigned molecular formulas. This example shows the simulated position and intensity of the $C_6H_9N_6^+$ ion (left part of the graph) and its isotopic signature (right part of the graph). The agreement between simulated position and relative intensities and the spectrum (dotted line), clearly demonstrates the validity of the molecular formula assignments.

that HCN polymer is more complex than a simple repetition of HCN elements. The ions present in positive and negative modes have mostly different molecular formula, and the use of the two complementary polarities gives us a more precise overview of the whole polymer. This comes from the ionization method that adds or removes a proton to the molecule and is controlled by the ability of the molecule to gain or lose a proton (i.e. the chemical functions that are present in the molecule and that can be protonated or deprotonated respectively in positive and negative mode).

Though simpler than tholins [12], the HCN polymer is composed of at least 1723 different molecular ions among which 1337 are mono-isotopic from the positive spectrum and 325 different molecules with 262 mono-isotopic from the negative spectrum.

3.3.2. Isotopic signatures a tool for assignment validation

A further proof of the validity of the molecular formula assignments is given by the isotopic signature of the most intense peaks in the spectrum. Fig. 4 shows the simulated position of the $C_6H_9N_6^+$ molecular ion (left part of Fig. 4) and its simulated isotopic signatures (right part of Fig. 4). Our simulation includes the carbon and nitrogen isotopes. As both mono-isotopic and isotopic signatures match with the spectra (solid line) both in exact mass and in relative intensities (though there is a symmetric under measurement of small peaks) of the isotopic peaks, it confirms that the assigned molecular formula is correct. The agreement of isotopic patterns has been positively checked in the same way for the 10 most intense peaks of the positive spectrum as a high signal to noise ratio is mandatory to see the isotopic peaks.

3.3.3. Interpretation of the molecular formulae

Once molecular formulae have been assigned to the peaks, a modified Van Krevelen diagram (used in petroleomics, [40]), shown in Fig. 5 for the molecular formulae derived for the positive ions and Fig. 6 for the negative ions, can be used to visualize all of the mono-isotopic peaks. A modified Van Krevelen diagram plots the H/C ratio versus the N/C ratio. The red circle close to the center of the graph represents the averaged H/C = 1.28 and N/C = 1.05 ratios, with an intensity weighting, of all the points in the diagram. The blue triangle represents the expected H/C and N/C ratios from elemental analysis and the pink square corresponds to the averaged H/C and N/C ratios with no weighting. Fig. 6 displays the same representation of the data set for the negative mode. The distribution in mass and the

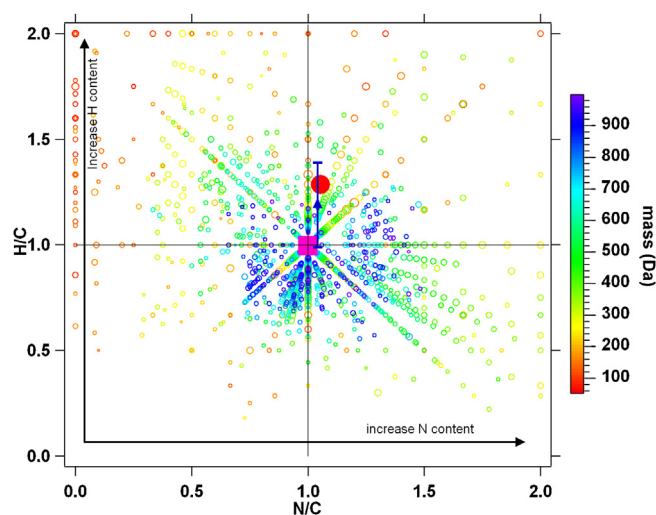


Fig. 5. Modified Van Krevelen diagram showing the H/C ratio versus the N/C ratio of all the mono-isotopic peaks identified in the positive ion spectrum. This diagram clearly shows that as the molecular mass increases, the H/C and N/C ratios tend toward a value of 1. The linear trends toward the coordinates (1;1) observed on this plot represent families of molecules. The size of the circles represents the intensity of the peak in the spectrum. The red circle close to the center of the graph represents the averaged N/C and H/C ratios with an intensity weighting and the pink square represents the average without weighting. The blue triangle represents the N/C and H/C ratios expected from the elemental analysis with the error bars (for N/C within the marker size). (For interpretation of the references to color in this figure legend, the reader is referred to the web version of this article.)

organization of the molecules around the point (1;1) is the same as for the positive mode. The red circle close to the center of the graph represents the averaged H/C = 0.920 and N/C = 1.008 ratios, with an intensity weighting, of all the points in the diagram. The averaged (taking into account both negative and positive modes) ratios are H/C = 1.1 and N/C = 1.029 and are in relatively good agreement with the elemental analysis of the polymer considering the small amount

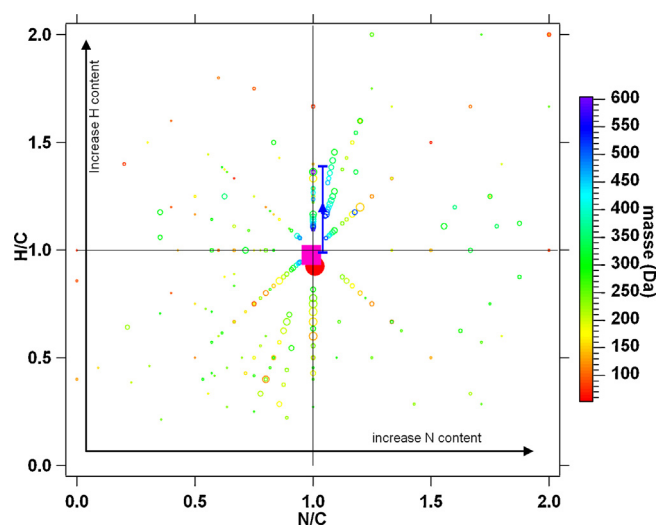


Fig. 6. Modified Van Krevelen diagram showing the H/C ratio versus the N/C ratio of all the mono-isotopic peaks identified in the negative ion spectrum. This diagram clearly shows that as the molecular mass increases, the H/C and N/C ratios tend toward a value of 1. The linear trends toward the coordinates (1;1) observed on this plot represent families of molecules. The size of the circles represents the intensity of the peak in the spectrum. The red circle close to the center of the graph represents the averaged N/C and H/C ratios with an intensity weighting and the pink square shows the average without weighting. The blue triangle represents the N/C and H/C ratios from the elemental analysis with the error bars (for N/C within the marker size). (For interpretation of the references to color in this figure legend, the reader is referred to the web version of this article.)

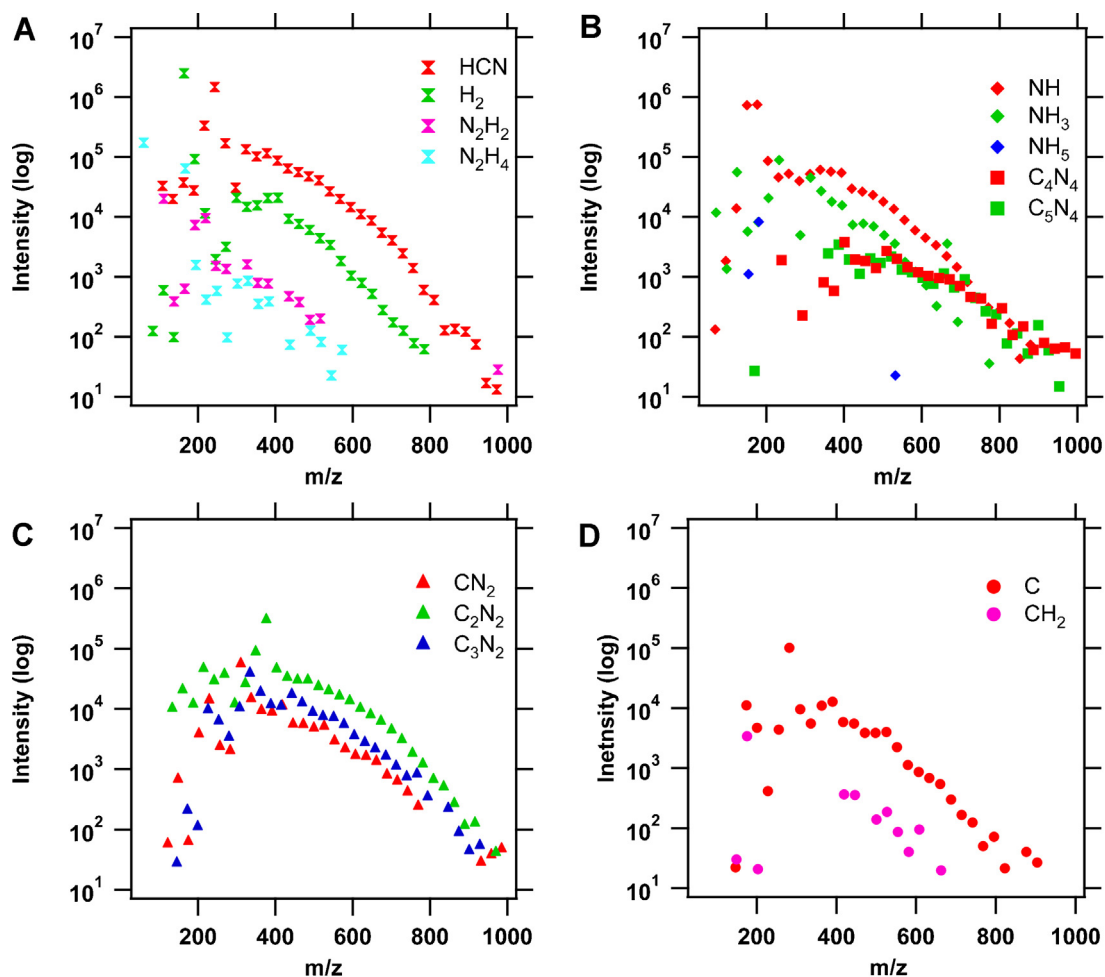


Fig. 7. Intensity versus mass of the 14 most intense identified families. The important observation is that their presence throughout the entire mass range validates their detection (i.e. they are not an assignment artifact). The shape of the intensity distribution versus the mass of all the molecules within each family follows the general distribution shown in Fig. 2.

of negatively charged ions identified. The pink square at the center of the graphs represents the averaged N/C and H/C ratios with no weighting. Those two different ways to calculate the averaged values (with or without weighting) demonstrates the relevance of the information contained in the intensity. The fact that we reach a value close to the one given by the elemental analysis means that intensity of the peaks mostly comes from the abundance of the molecules in the sample. Considering the fact that the number of molecules is huge in positive ionization mode compare to the negative ion mode and that the elemental analysis was performed on the whole polymer, we calculate the averaged H/C and N/C ratios of the whole polymer (negative and positive) weighted by the number of molecules. The weighting is done by weighting the average ratios in positive and negative mode (weighted by the intensities of the peaks) by the number of molecules detected in both modes. This calculation results in H/C = 1.22 (H/C = 1.19 from elemental analysis) and N/C = 1.04 (N/C = 1.04 from elemental analysis).

It is clear that as the molecular mass increases, both ratios tend toward a value of 1 as it can be expected for HCN polymer resulting from HCN addition. In those Van Krevelen diagrams the H/C and N/C patterns can be fitted linearly toward the point (1;1). The observed linear patterns (all converging toward the point (1;1) on this diagram) are not coincidental; they represent families of molecules, the members of which are separated by the exact mass of HCN (27.0108 Da). The molecular formulae can be rewritten based on those families. For example the molecule $C_6H_9N_7$ can therefore be rewritten as $(HCN)_6 NH_3$ and will therefore belong to the $(HCN)_x$

NH_3 family (with an x value that varies between 2 and 37 in our spectra). As the repetitive pattern of a family is identified, we can look for this family through the entire mass range.

Fig. 7 shows the evolution of intensity of the 14 most intense families (among 243) that have been identified in positive mode and are summarized in Table 2. The family detections are validated by the distribution of the intensities as a function of the mass; for

Table 2

The 14 most intense identified families in positive mode are shown here with the respective number of members and the identity of the most intense member.

Family	Identified members	Most intense member		
		Formula	Measured mass (m/z)	x in family
$(HCN)_x$	35	$C_9H_{10}N_9^+$	244.1055	9
$(HCN)_xCH_2$	13	$C_7H_9N_6^+$	177.0885	6
$(HCN)_xCN_2$	28	$C_{11}H_{11}N_{12}^+$	311.1226	10
$(HCN)_xC_2N_2$	31	$C_{14}H_{13}N_{14}^+$	377.1441	12
$(HCN)_xC$	31	$C_{11}H_{11}N_{10}^+$	283.1166	10
$(HCN)_xC_3N_2$	29	$C_{13}H_{10}N_{12}^+$	335.1405	10
$(HCN)_xC_4N_4$	28	$C_{15}H_{12}N_{15}^+$	402.1390	11
$(HCN)_xC_5N_4$	24	$C_{15}H_{11}N_{14}^+$	387.1283	10
$(HCN)_xH_2$	30	$C_6H_7N_6^+$	165.0883	6
$(HCN)_xNH$	30	$C_6H_8N_7^+$	178.0836	6
$(HCN)_xNH_3$	24	$C_8H_{12}N_9^+$	234.1211	8
$(HCN)_xNH_5$	5	$C_6H_{12}N_7^+$	182.1149	6
$(HCN)_xN_2H_2$	15	$C_3H_6N_5^+$	113.0615	3
$(HCN)_xN_2H_4$	16	$C_1H_6N_3^+$	60.0551	1

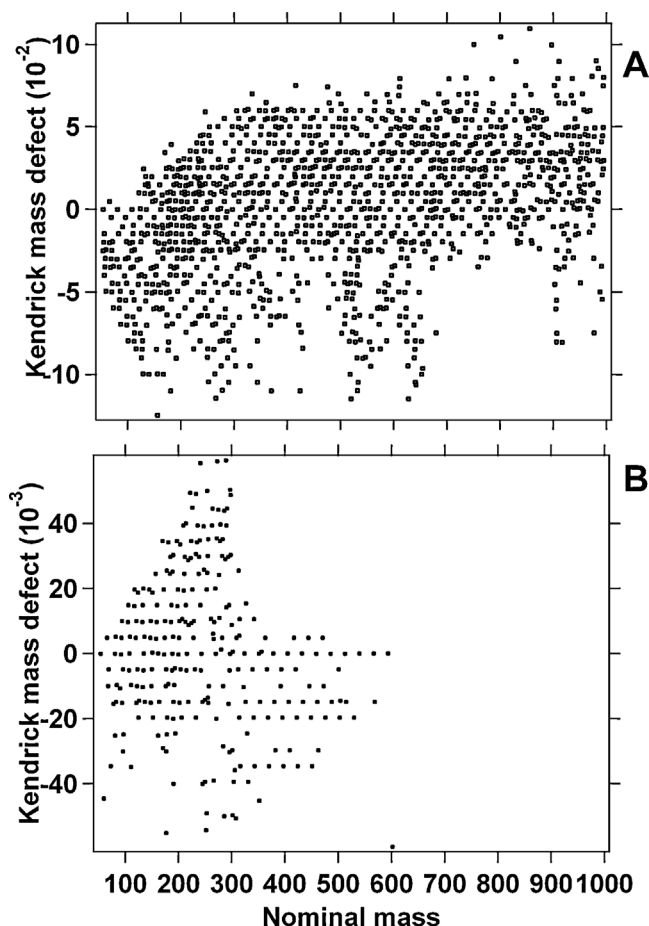


Fig. 8. Panel A represents the evolution of the HCN Kendrick mass defect for the identified molecular formulae in the positive ion mode data. Panel B represents the evolution of the HCN Kendrick mass defect for the identified molecular formulae in the negative ion mode data. This representation of the data set allows us to identify HCN as the basic molecular building block as extended horizontal lines are drawn.

all the families it follows the general distribution shown in Fig. 2 (essentially depending on instrumental transmission and ionization efficiency). The identification of those families is the same for the negative mode even if fewer molecules have been identified. Since the molecules in a given family are separated by the exact mass of HCN, HCN monomer seems to be the repetitive pattern involved as a molecular building block.

This observation is corroborated by the (HCN) Kendrick mass defect diagram shown in Fig. 8A for the positive ions and Fig. 8B for the negative ions. This diagram shows the evolution of the Kendrick mass defect versus the exact Kendrick mass that corresponds to the normalization of the exact measured mass to fit with a repetitive pattern of normalized mass. For instance, it is possible

to use a HCN mass of 27 instead of 27.0108, using Eqs. (1) and (2) from [41].

$$\text{Exact Kendrick mass} = \text{Exact measured mass} * \left(\frac{27}{27.0108} \right) \quad (1)$$

$$\text{Kendrick mass defect} = (\text{nominal mass} - \text{exact Kendrick mass}) \quad (2)$$

The nominal mass is the entire fraction of the exact mass. Several patterns have been tested CH₂, NH₃, CH₂NH (not shown) and HCN. The repetitive pattern is found to be HCN as it is the one that draws the most extended horizontal lines.

The huge matrix built up by all the family roots can be simplified; all the roots can be constructed by a combination of 4 components that are NH, C, N₂ and H₂. Nevertheless, even if 243 different families have been identified in the spectrum, some families are absent. Hence, the number of H or N atoms in the root is never odd when associated to whatever carbon number. When both H and N appear in the root, it is the sum of their number of atoms that is never odd. This correlates to the so-called “nitrogen rule” and explicitly shows that the ions detected, though very complex and encompassing a great variety, are never radical ions.

All the families are sharing a repetitive pattern of HCN addition; they are globally in agreement with the polyimine structure identified by He et al. [31]. Formally, the (HCN)_x family, which is the most intense, is in perfect agreement with the main structure they proposed. Other families correspond to combinations of saturation, unsaturation or insertions of small molecular structures (either C or NH) in the molecular chain, which can occur in the course of the polymerization process. It is important here to note that the deviation from the canonical (HCN)_x pattern is hence very limited.

3.3.4. Structural analysis and tandem mass spectrometry (MS/HRMS)

While the patterns observed in the molecular formulae can provide insight into the general organization of the polymer, the understanding of the molecular structures which are present in the sample provides additional constraints on its chemical diversity. To do that, tandem mass spectrometry (MS/MS) with the Orbitrap as a final analyzer (High resolution: MS/HRMS) was used. This kind of study was previously described by Neish et al. [26] to identify structures in hydrolyzed tholins.

Tandem mass spectrometry or MS/HRMS was used to investigate the structure of eight molecules contained in the HCN polymer. Those ions were selected because their intensity is high enough to see the fragment peaks in the spectrum, except for C₆H₁₁N₈⁺ (*m/z* = 195) which was chosen because the mass of the most intense ion in its family (guanidine CH₆N₃ at *m/z* = 60) was too low to record the fragmentation spectrum. Fig. 9 presents the results of MS/HRMS experiments for the eight ions investigated here (summarized in Table 3). The major fragment for C₆H₉N₆⁺ (*m/z* = 165), C₆H₈N₇⁺ (*m/z* = 178), C₇H₁₀N₇⁺ (*m/z* = 192), C₆H₁₁N₈⁺ (*m/z* = 195), C₈H₉N₈⁺

Table 3

List of the ions studied by MS/HRMS with their respective molecular formula, relative difference compared to theoretical exact mass, assigned family and most intense lost fragment.

Parent ion exact mass	Formula	Δ (ppm)	Family	Value of x in family	Major fragment lost
<i>m/z</i> = 109.0506	C ₄ H ₅ N ₄ ⁺	−2.6	(HCN) _x	4	HCN
<i>m/z</i> = 217.0944	C ₈ H ₉ N ₈ ⁺	−2.7	(HCN) _x	8	NH ₃ and HCN
<i>m/z</i> = 244.1055	C ₉ H ₁₀ N ₉ ⁺	+0.35	(HCN) _x	9	NH ₃
<i>m/z</i> = 165.0882	C ₆ H ₉ N ₆ ⁺	−0.58	(HCN) _x H ₂	6	NH ₃
<i>m/z</i> = 178.0833	C ₆ H ₈ N ₇ ⁺	−1.2	(HCN) _x NH	6	NH ₃
<i>m/z</i> = 192.0989	C ₇ H ₁₀ N ₇ ⁺	−1.4	(HCN) _x H ₂	7	NH ₃
<i>m/z</i> = 195.1096	C ₆ H ₁₁ N ₈ ⁺	−2.7	(HCN) _x N ₂ H ₄	6	NH ₃
<i>m/z</i> = 261.1320	C ₉ H ₁₃ N ₁₀ ⁺	+1.3	(HCN) _x NH ₃	9	NH ₃

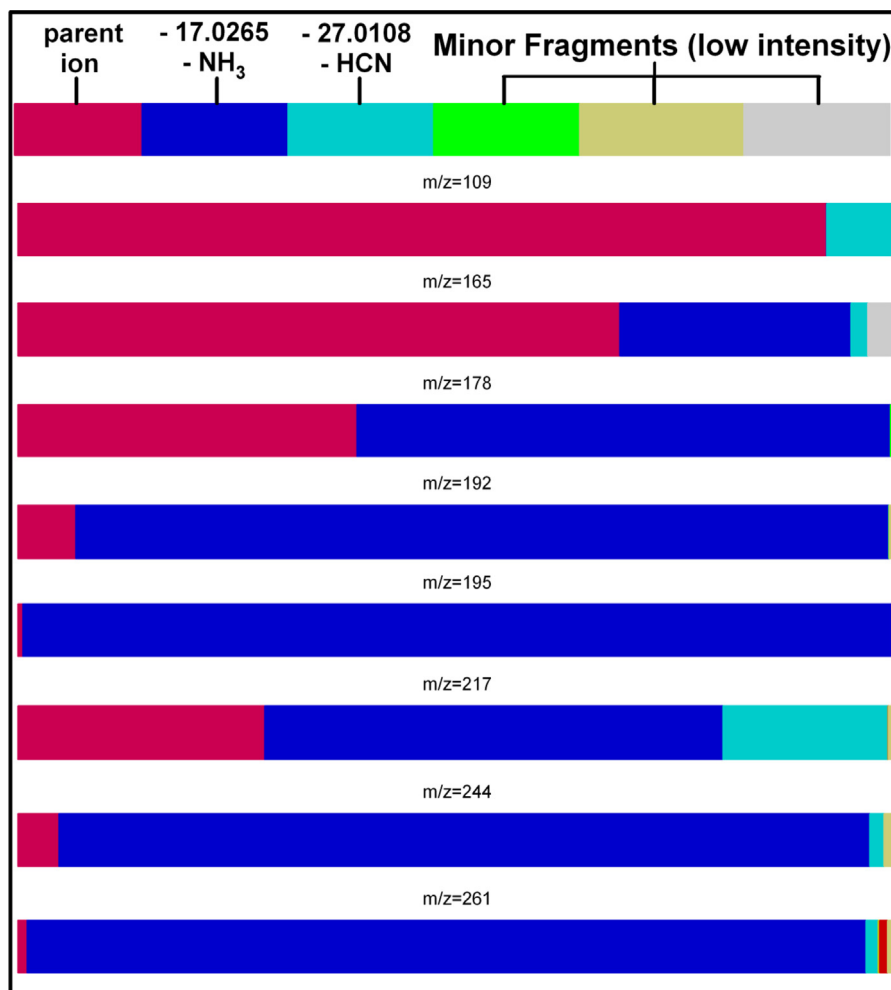


Fig. 9. MS/HRMS results for the eight studied ions. The color corresponds to molecular fragments as shown in the figure. The length of the colored zone corresponds to the relative intensity of the peak in the spectrum. (For interpretation of the references to color in this figure legend, the reader is referred to the web version of this article.)

($m/z = 217$), $C_9H_{10}N_9^+$ ($m/z = 244$) and $C_9H_{13}N_{10}^+$ ($m/z = 261$) is NH_3 while for $C_4H_4N_4^+$ ($m/z = 109$) the main loss observed is that of HCN.

This clearly demonstrates that amines are present as a significant fraction in HCN polymer, once again in agreement with the description of small molecular structure identified by He et al. [31]. But ions at $m/z = 109$, 217 and 244 (that all belong to the same $(HCN)_x$ family, with $x = 4$, 8 and 9, respectively) do not exhibit identical fragmentation patterns. This indicates a more complex evolution within a given family of molecules; a simple linear polymerization scheme is not valid. Rather reorganization of the structure seems to happen during the polymerization process. This is consistent with the TMAH (tetramethylammonium hydroxide) thermochemolysis/GCMS study of Minard et al. [19] that demonstrates the presence of N bearing heterocycles in HCN polymer, which are not formed by simple monomer addition. It is also consistent with the work of Matthews and Minard [22] who proposed a pathway for building ring structures during the polymerization. In addition the fragmentation pattern of $C_4H_5N_4^+$ ($m/z = 109$), which has a low fragmentation efficiency, shows that the structure is resistant to the collision induced dissociation, which may indicate the presence of an aromatic ring in the structure.

Further interpretation of the fragmentation pattern requires the use of standard molecules. Accordingly we have acquired fragmentation spectra of pure standards and compared them with spectra of HCN polymer. The ion $C_4H_5N_4^+$ at $m/z = 109$ corresponding to the $C_4H_5N_4^+$ formula is of great interest as previous studies have

suggested that the tetramer of HCN is an important intermediate in the polymerization process [31,42,43]. Fig. 10 shows the fragmentation pattern of $m/z = 109$ in the HCN polymers (panel A) and three standard molecules at the same mass (panel B and C) with the same molecular formula, but of known structure, diamino-maleonitrile (DAMN), 4(5)-Amino-1H-imidazole-5(4)-carbonitrile, and 3-Amino-4-cyanopyrazole respectively. This figure shows that those three isomers are not present in HCN polymer, in significant amount, because their fragmentation patterns do not match the spectrum of the HCN polymer. This is consistent with the observation of [44] that DAMN is a crystalline product during the polymerization and that it is not soluble in liquid HCN. The low fragmentation efficiency of the HCN polymer ion is consistent with an aromatic ring structure linked to a short chain. Let us note that this technique of dissociation to elucidate structure of unknown ions is limited by the fact that the HCN polymer may not be isomerically pure, which implies that several isomers can be present at a given exact mass. Thus the fragmentation spectrum of HCN polymers could be the combination of the fragmentation patterns of multiple isomers. As a consequence we can just conclude that DAMN is not the major ion at $m/z = 109$.

Nevertheless, iterative MS/MS spectra can reveal the structure of a given molecule through successive removal of chemical functional groups that constitute the molecular backbone. With this aim, the iterative MS/MS spectra of the $m/z = 244$ molecule ($C_9H_{10}N_9^+$ from the $(HCN)_x$ family), is of great interest.

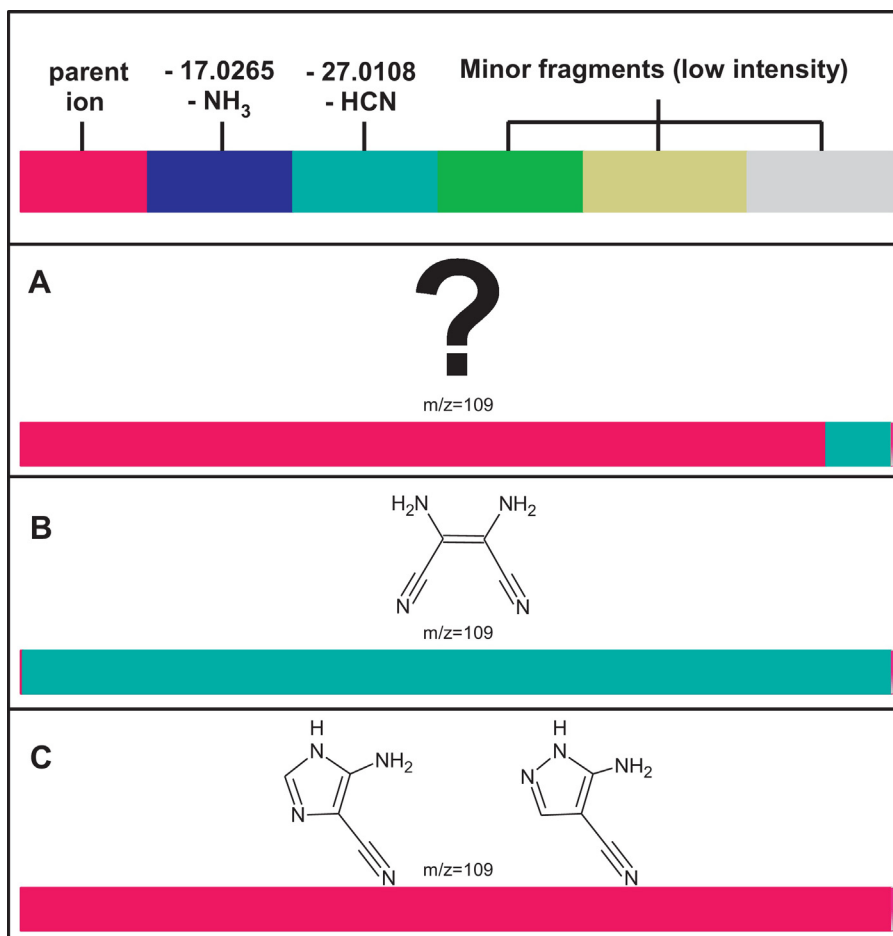


Fig. 10. Comparison between the fragmentation patterns of $m/z = 109$ in the HCN polymer (panel A) and three standard molecules: diaminomaleonitrile (DAMN) (panel B), the 4(5)-amino-1H-imidazole-5(4)-carbonitrile and the 3-amino-4-cyanopyrazole respectively (panel C). This clearly demonstrates that none of these three standards is the correct isomer. However the polymer may not be pure isomeric material and the fragmentation pattern of its $m/z = 109$ ion(s) is may be a combination of multiple isomer signatures. The color code is the same as for Fig. 9. (For interpretation of the references to color in this figure legend, the reader is referred to the web version of this article.)

The succession of fragmentations is shown in Fig. 11. The first parent ion selected is $C_9H_{10}N_9^+$, the most intense peak in the spectrum (i.e. $m/z = 244$). The high fragmentation efficiency is consistent with an elongated structure; the main fragment is NH_3 which is consistent with a chain containing amine groups.

This is also consistent with the strong signatures of amine in the infrared spectrum of the HCN polymer. Then the lighter ion, $C_9H_7N_8$ at $m/z = 227$ ($C_9H_8N_8^+$: $m/z = 244 - NH_3$) is selected, becoming the new parent ion, and broken. This ion has lower fragmentation efficiency and the main fragment is HCN. For the

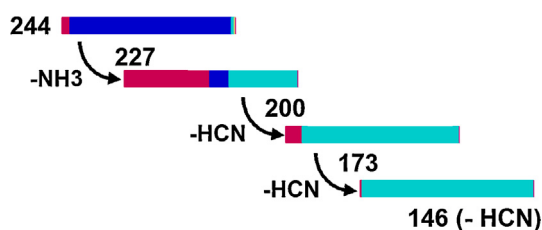


Fig. 11. Successive MS/MS from the initial parent ion at $m/z = 244$ and its lighter daughter ions at $m/z = 227$, 200 and 173). This iterative measurement demonstrates that HCN polymer molecules contain chains built up by HCN monomers (HCN loss) and containing amine groups (initial intense loss of NH_3 from $m/z = 244$). The measurements ended when the signal to noise ratio became too low while trying to fragment the ion at $m/z = 146$. The color code is the same as for Figs. 9 and 10. (For interpretation of the references to color in this figure legend, the reader is referred to the web version of this article.)

two next ions, $m/z = 200$ ($C_8H_6N_7^+$: $m/z = 227 - HCN$) and $m/z = 173$ ($C_7H_5N_6^+$: $m/z = 200 - HCN$), the only fragment is HCN. The molecular backbone then seems to be constructed of HCN monomers. The MS/HRMS experiment ended because the signal to noise ratio was too low when trying to break the ion $C_6H_4N_5^+$ ($m/z = 146$). Finally, the conclusion of this iterative MS/MS measurement is that HCN polymer molecules seem to have a backbone constituted by HCN monomer. Then reorganization can occur to form aromatic rings even at low mass ($C_4H_5N_4^+$: $m/z = 109$). Additionally, the aromatic rings can be linked to chains of various lengths that have amine groups. Aromatics are also supported by the distribution of the heavy atoms as a function of the mass ($(C+N)/mass$). Almost all the molecules lie between 0.5 and 1 and that means that the polymer molecules are highly unsaturated. The unsaturation carrier is conjugated chains like imines and also aromatics.

4. Conclusion

In conclusion, high resolution mass spectrometry is a very sensitive and suitable technique to study complex organic molecules [32] and thus HCN polymers. This technique gives results in good agreement with previous studies: NMR [27] and TMAH/GCMS [22]. This technique is also of great interest for trying to interpret and understand the structures of molecules present in HCN polymers. The use of tandem mass spectrometry allows for deeper characterization of the molecules present in HCN polymer than is

possible through the use of mass spectrometry alone and can be used as a tool to confirm or invalidate structures. It has been shown that molecules are constituted by HCN monomers and that chains have amine groups. It has also been shown that aromatic rings are probably present in HCN polymers. In this study, comparison of the fragmentation pattern of HCN polymers and standard molecules is a key step in understanding fragmentation processes by providing insight into the behavior of different chemical functional groups during MS/HRMS.

This is the first extended study to use very high resolution mass spectrometry to analyze HCN polymer and additional analytical efforts should provide further insight into the composition of HCN polymers. In this way the use of liquid chromatography coupled with high resolution mass spectrometry could be of great interest for deeper discrimination between different isomers. Study of laboratory analogs of planetary organic materials through the use of mass spectrometry is necessary for accurate interpretation of the low resolution mass spectrometry data obtained by current spacecraft and also for development of future high resolution flight instruments.

Acknowledgements

This work was supported by ANR-07-BLAN-0123, Cible 2007 of Rhône-Alpes Region, CNES Astrobiology/Exobiology, and the CNRS program Origines Planètes Vie (OPV). Véronique Vuitton is grateful to the European Commission for the Marie Curie International Reintegration Grant No. 231013. Lena Le Roy is the recipient of a CNES/Région Centre grant for her PhD work. Sarah M. Hörst is supported by a NSF Astronomy and Astrophysics Postdoctoral Fellowship AST-1102827. Sarah M. Hörst and Roger V. Yelle are supported by a NASA Planetary Atmospheres Grant NNX09AB586 and JPL subcontract 1372177 under the NASA Astrobiology Institute.

References

- [1] A.M.S. Boonman, R. Stark, E.F. van der Tak, E.F. van Dishoeck, P.B. van der Wal, F. Schäfer, G. de Lange, W.M. Laauwen, Highly abundant HCN in the inner hot envelope of GL 2591: probing the birth of a hot core? *The Astrophysical Journal* 553 (2001) L63–L67.
- [2] P. Ehrenfreund, S.B. Charnley, Organic molecules in the interstellar medium, comets and meteorites: a voyage from dark clouds to the early earth, *Annual Review of Astronomy and Astrophysics* 38 (2000) 427–483.
- [3] J.R. Pardo, J. Cernicharo, J.R. Goicoechea, Observational evidence of the formation of cyanopolynes in CRL 618 through the polymerization of HCN, *The Astrophysical Journal* 628 (2005) 275–282.
- [4] F. Woeller, G. Ponnampereuma, Organic synthesis in a simulated Jovian atmosphere, *Icarus* 10 (1969) 386–392.
- [5] G.A. Baratta, G. Strazzulla, Ion produced Organic Cometary Crust, Asteroids, Comets, Meteors, Lunar and Planetary Institute, Houston, 1991, pp. 41–44.
- [6] D.P. Cruikshank, L.J. Allamandola, W.K. Hartmann, D.J. Tholen, R.H. Brown, C.N. Matthews, J.F. Bell, Solid CN bearing material on outer solar system bodies, *Icarus* 94 (1991) 345–353.
- [7] T.W. Rettig, S.C. Tegler, D.J. Pasto, M.J. Mumma, Comet outburst and polymer of HCN, *The Astrophysical Journal* 398 (1992) 293–298.
- [8] G. Strazzulla, Ion irradiation experiments and nitrogen bearing species on Jovian and Saturnian icy surfaces, *Planetary and Space Sciences* 47 (1999) 1371–1376.
- [9] H. Imanaka, M.A. Smith, Formation of nitrogenated organic aerosols in the Titan upper atmosphere, *Proceedings of the National Academy of Sciences* 107 (2010) 12423–12428.
- [10] C.N. Matthews, Hydrogen cyanide polymers from the impact of comet shoemaker levy on Jupiter, *Advances in Space Research* 19 (1997) 1087–1091.
- [11] D.E. Budil, J.L. Roebber, S.A. Liebman, C.N. Matthews, Multifrequency electron spin resonance detection of solid-state organic free radicals in HCN polymer and a Titan tholin, *Astrobiology* 3 (2003) 323–329.
- [12] V. Vuitton, J.-Y. Bonnet, M. Frisari, R. Thissen, E. Quirico, O. Dutuit, B. Schmitt, L. Le Roy, N. Fray, H. Cottin, E. Sciamma-O'Brien, N. Carrasco, C. Szopa, Very high resolution mass spectrometry of HCN polymers and tholins, *Faraday Discussions* 147 (2010) 495–508.
- [13] N. Fray, Etude expérimentale et théorique de la contribution de la composante organique réfractaire à la phase gazeuse dans l'environnement cométaire, Université Paris XII, 2004 (PhD thesis).
- [14] N. Fray, Y. Bénilan, H. Cottin, M.-C. Gazeau, J. Crovisier, The origin of the CN radical in comets: a review from observations and models, *Planetary and Space Sciences* 53 (2005) 1243–1262.
- [15] H. Cottin, N. Fray, Distributed sources in comets, *Space Science Reviews* 138 (2008) 179–197.
- [16] S.A. Sandford, J. Aléon, C.M.O'D. Alexander, T. Araki, S. Bajt, G.A. Baratta, J. Borg, J.P. Bradley, D.E. Brownlee, J.R. Brucato, M.J. Burchell, H. Busemann, A. Butterworth, S.J. Clemett, G. Cody, L. Colangeli, G. Cooper, L. D'Hendecourt, Z. Djouadi, J.P. Dworkin, G. Ferrini, H. Fleckenstein, G.J. Flynn, I.A. Franchi, M. Fries, M.K. Gilles, D.P. Glavin, M. Gounelle, F. Grossemy, C. Jacobsen, L.P. Keller, A.L.D. Kilcoyne, J. Leitner, G. Matrajt, A. Meibom, V. Mennella, S. Mostefaoui, L.R. Nittler, M.E. Palumbo, D.A. Papanastassiou, F. Robert, A. Rotundi, C.J. Snead, M.K. Spencer, F.J. Stadermann, A. Steele, T. Stephan, P. Tsou, T. Tylliszczak, A.J. Westphal, S. Wirick, B. Wopenka, H. Yabuta, R.N. Zare, M. Zolensky, Organics captured from Comet 81P/Wild 2 by the Stardust spacecraft, *Science* 314 (2006) 1720.
- [17] M.C. Festou, H.U. Keller, H.A. Weaver, *Comets II*, University of Arizona Press, Tucson, Arizona, 2004.
- [18] D. Despois, J. Crovisier, D. Bockelee-Morvan, J. Schraml, T. Foreveille, E. Gerard, Observations of hydrogen cyanide in comet halley, *Astronomy and Astrophysics* 160 (1986) L11–L12.
- [19] R.D. Minard, P.G. Hatcher, R.C. Gourley, C.N. Matthews, Origins of life and evolution of the biosphere 28 (1998) 461–473.
- [20] S.A. Liebman, R.A. Pesce-Rodriguez, C.N. Matthews, Organic analysis of hydrogen cyanide polymers: prebiotic and extraterrestrial chemistry, *Advances in Space Research* 15 (1995) 71–80.
- [21] C.N. Matthews, R.D. Minard, Hydrogen cyanide polymers, comets and the origin of life, *Chemical Evolution of the Universe: Faraday Discussions* 133 (2006) 393–401.
- [22] C.N. Matthews, R.D. Minard, Hydrogen cyanide polymers connect cosmochemistry and biochemistry, *Proceedings IAU Symposium* 251 (2008) 453–458.
- [23] C.N. Matthews, R.E. Moser, Prebiological protein synthesis, *Proceedings of the National Academy of Sciences of the United States of America* 56 (1966) 1087–1094.
- [24] C.N. Matthews, R.E. Moser, Peptide synthesis from hydrogen cyanide and water, *Nature* 215 (1967) 1230–1234.
- [25] I. Mamajanov, J. Herzfeld, HCN polymers characterized by solid state NMR: chains and sheets formed in the neat liquid, *Journal of Chemical Physics* 130 (2009) 134503.
- [26] C.D. Neish, A. Somogyi, M.A. Smith, Titan's primordial soup: formation of amino acids via low-temperature hydrolysis of tholins, *Astrobiology* 10 (3) (2010) 337–347.
- [27] J.R. Garbow, J. Schaefer, R. Ludicky, C.N. Matthews, Detection of secondary amides in HCN polymers by dipolar rotational spin-echo ^{15}N NMR, *Macromolecules* 20 (1987) 305–309.
- [28] C.N. Matthews, R. Ludicky, Heteropolypeptides from hydrogen cyanide and water? Solid state ^{15}N NMR investigations, *Origins of Life* 14 (1984) 243–250.
- [29] R.A. McKay, J. Schaefer, E.O. Stejskal, Double-cross-polarization detection of labeled chemical bonds in HCN polymerization, *Macromolecules* 17 (1984) 1124–1130.
- [30] J. Schaefer, E.O. Stejskal, G.S. Jacob, R.A. McKay, Natural abundance N-15 NMR of the solids from the reaction of HCN and ammonia, *Applied Spectroscopy* 36 (1982) 179–182.
- [31] C. He, G. Lin, K.T. Upton, H. Imanaka, M.A. Smith, Structural investigation of HCN polymer isotopomers by solution state multidimensional NMR, *Journal of Physical Chemistry A* 116 (2012) 4751–4759.
- [32] N. Sarker, A. Somogyi, J.I. Lunine, M.A. Smith, Titan aerosol analogues: analysis of the nonvolatile tholins, *Astrobiology* 3 (2003) 719–726.
- [33] C.L. Ricketts, D. Schroeder, C. Alcaraz, J. Roithova, Growth of larger hydrocarbons in the ionosphere of Titan, *Chemistry: A European Journal* 14 (16) (2008) 4779–4783.
- [34] D. Ascenzi, J. Roithova, D. Schroeder, E.L. Zins, C. Alcaraz, Growth of doubly ionized C₂H₅⁺ compounds in the presence of methane, *Journal of Physical Chemistry A* 113 (42) (2009) 11204–11210.
- [35] J. Zabka, M. Polasek, D. Ascenzi, P. Tosi, J. Roithova, D. Schroeder, Reactivity of C₂H₅⁺ with benzene: formation of ethylbenzenium ions and implications for Titan's ionospheric chemistry, *Journal of Physical Chemistry A* 113 (42) (2009) 11153–11160.
- [36] E.L. Zins, D. Schroeder, Carbon-carbon coupling reactions of medium-sized nitrogen-containing dications, *Journal of Physical Chemistry A* 114 (19) (2010) 5989–5996.
- [37] C. Szopa, G. Cernogora, L. Boufendi, J.J. Correia, P. Coll, PAMPRE: a dusty plasma experiment for Titan's tholins production and study, *Planetary and Space Sciences* 54 (2006) 394–404.
- [38] N. Carrasco, I. Schmitz-Afonso, J.-Y. Bonnet, E. Quirico, R. Thissen, O. Dutuit, A. Bagag, O. Laprèvote, A. Buch, A. Giuliani, G. Adandé, F. Ouni, E. Hadamcik, C. Szopa, G. Cernogora, Chemical characterization of Titan's tholins: solubility, morphology and molecular structure revisited, *Journal of Physical Chemistry A* 113 (2009) 11195–11203.
- [39] S.M. Hörst, Post-Cassini investigations of Titan atmospheric chemistry, University of Arizona, Tucson, 2011 (Ph.D. thesis).

- [40] Z. Wu, R.P. Rodgers, A.G. Marshall, Two- and three-dimensional van Krevelen diagrams: a graphical analysis complementary to the Kendrick mass plot for sorting elemental compositions of complex organic mixtures based on ultrahigh-resolution broadband Fourier transform ion cyclotron resonance mass measurements, *Analytical Chemistry* 76 (2004) 2511–2516.
- [41] C.A. Hughey, C.L. Hendrickson, R.P. Rodgers, A.G. Marshall, K. Qian, Kendrick mass defect spectrum: a compact visual analysis for ultrahigh-resolution broadband mass spectra, *Analytical Chemistry* 73 (2001) 4676–4681.
- [42] R. Minard, W. Yang, P. Varma, J. Nelson, C.N. Matthews, Heteropolypeptides from poly alpha-cyanoglycine and hydrogen cyanide – model for origin of proteins, *Science* 190 (1975) 387–389.
- [43] C.N. Matthews, Hydrogen cyanide polymers: from laboratory to space, *Planetary and Space Sciences* 43 (1995) 1365–1370.
- [44] R.E. Moser, A.R. Claggett, C.N. Matthews, Peptide formation from diamino-maleonitrile (HCN tetramer), *Tetrahedron Letters* 9 (1968) 1599–1603.